Research article

Energy efficient resource allocation of IRS-Assisted UAV network

Shuang Zhang[1,2]**, Songwen Gu**[1]**, Yucong Zhou**[1]**, Lei Shi**[3] **and Huilong Jin**[1,4,*]

[1] Hebei Normal University, Shijiazhuang 050024, China

[2] Hebei Provincial Key Laboratory of Information Fusion and Intelligent Control, Shijiazhuang 050024, China

[3] Key Laboratory of Education Informatization for Nationalities, Yunnan Normal University, Ministry of Education, Kunming 650092, China

[4] Hebei Provincial Innovation Center for Wireless Sensor Network Data Application Technology, Shijiazhuang 050024, China

* **Correspondence:** Email: JHL981@hebtu.edu.cn.

Abstract: The integration of unmanned aerial vehicle (UAV) networks with intelligent reflecting surface (IRS) technology offers a promising solution to enhance wireless communication by dynamically altering signal propagation. This study addresses the challenge of maximizing system energy efficiency (EE) in IRS-assisted UAV networks. The primary objective is to optimize power allocation and IRS reflection design to achieve this goal. To tackle the optimization problem, we employ a block coordinate descent (BCD) method, decomposing it into three subproblems: phase shift optimization, power allocation, and trajectory planning. These subproblems are iteratively solved using an improved particle swarm optimization (PSO) algorithm. Simulation results demonstrate that the proposed PSO algorithm effectively plans high-quality UAV trajectories in complex environments, significantly enhancing EE. The findings suggest that the IRS-assisted UAV model outperforms traditional UAV models, offering substantial improvements in wireless communication quality and EE.

Keywords: UAV; IRS; EE; power allocation; trajectory optimization; PSO

1. Introduction

1.1. Background

Unmanned aerial vehicles (UAVs), which are aircraft with autonomous flying capabilities, have gained popularity due to their low cost, high flexibility, and ease of deployment. Compared with

ground communication, UAVs have a higher probability of establishing line-of-sight (LoS) communication links, resulting in superior channel quality. Efficient UAV path planning is essential to minimize energy consumption while meeting the user's signal rate requirements. The LoS probability is used to determine the optimal destination location where the UAV can maintain LoS with the user and provide the required downlink rate [1]. Meanwhile, the emerging intelligent reflecting surface (IRS) technology has become a promising solution for future wireless channels. Unlike traditional relay technology, IRS does not require power amplifiers and radio frequency chains, thus improving reliability with low power consumption and hardware cost. The quasi-passive nature of IRS allows it to be manufactured with lightweight and limited thickness, enabling easy installation on surfaces like buildings and ceilings [2]. IRS installed on high-rise buildings are more conducive to establishing LoS links with UAVs due to their higher altitudes and shorter distances, effectively avoiding obstacles [3]. This can enhance signal strength and mitigate eavesdropping, thereby improving spectrum efficiency and EE by establishing a virtual communication link. The basic principle of IRS involves reflecting incident signals and altering their phase shift to manipulate the wireless channel environment [4].

Despite the advantages of UAVs and IRS, the challenge of optimizing EE in UAV path planning remains unresolved. Deploying IRS to reconfigure the UAV communication propagation environment can significantly improve the coverage and performance of air-ground networks. However, before fully reaping the benefits of UAV wireless communication systems, it is crucial to address the issue of energy consumption [5]. The UAV path planning problem is a multivariate problem that considers many aspects comprehensively and seeks the optimal solution in a complex environment [6]. A path with strong security and good feasibility can greatly enhance the efficiency of UAV missions and maximize EE [7]. The path planning algorithm is the core of path planning, and optimization algorithms can accelerate convergence speed and improve search ability [8].

1.2. Related work and motivation

Existing research on IRS-assisted UAV communications can be categorized into two main approaches: traditional optimization algorithms and reinforcement learning (RL). Traditional algorithms include sequential convex approximation (SCA) [9–12], block coordinate descent (BCD) [13], genetic algorithms (GA) [14], and game theory [15]. For instance, Su et al. [9] equipped the IRS on a fixed-wing UAV and solved the problem of maximizing spectrum efficiency (SE) and EE through joint optimization of active beamforming at the base station, passive beamforming at the IRS, and the path of the UAV based on convex-concave algorithm. Song et al. [10] maximized the minimum average transmission rate by jointly optimizing communication scheduling, IRS phase shift, and UAV trajectory. Long et al. [11] proposed an iterative algorithm applying SCA and alternating optimization to jointly optimize the IRS phase and UAV trajectory. Ji et al. [12] used SCA and semi-definite relaxation algorithms to optimize ground node transmission power, and passive beamforming of IRS and UAV trajectory to maximize the average communication rate. Mu et al. [13] combined IRS with nonorthogonal multiple access (NOMA), optimizing UAV layout, transmit power, IRS transmit matrix, and NOMA decoding order using BCD. Shakhatreh et al. [14] used GA to find dynamic and effective UAV trajectories to maximize data rate and user power allocation. Diamanti et al. [15] applied game theory to optimize received signal strength and energy efficiency in a multi-user communication system, though it did not address continuous optimization problems.

RL methods are more effective in handling real-time, variable, and complex scenarios, requiring additional computing services. Zhang et al. [16] proposed a trajectory optimization method based on RL, optimizing resource allocation and IRS phase shift. Lin et al. [17] combined deep RL and linear programming for UAV-assisted mobile edge computing. Yu et al. [18] developed a deep learning (DL)-based channel tracking algorithm for IRS-assisted UAV communication systems. Abohashish et al. [19] proposed a load balancing scheme for UAV trajectory optimization based on RL. Ullah et al. [20] developed an RL-based method to optimize UAV trajectory and enhance LoS connection. Ejaz et al. [21] proposed an RL-based path planning method for UAV mobile edge computing networks. Wang et al. [22] studied an IRS-assisted UAV communication system, proposing deep Q network (DQN) and deep deterministic policy gradient (DDPG)-based algorithms for trajectory optimization.

Given the limited onboard energy of battery-powered UAVs, EE is a critical consideration. We aim to maximize the EE of passive IRS-assisted UAV communication with trajectory planning, resource allocation, and phase shift optimization. Based on existing algorithms and considering the limited energy of UAVs, we propose an iterative algorithm based on particle swarm optimization (PSO), which is more intelligent, simpler, and less computationally complex than SCA. The algorithm optimizes UAV trajectory, reduces flight distance, and lowers system energy consumption [23]. Compared with passive IRS, the extra power consumption of active IRS is related to direct current biasing power and phase shift power consumption, which are constants influenced by the number of IRS [24]. Therefore, our proposed algorithm is applicable for active IRS as well.

The key contributions of this paper are outlined as follows:

(1) A UAV information collection system based on passive IRS is proposed. Considering the mobility of ground users and interference from eavesdroppers, a new wireless communication channel for UAV is constructed using IRS, reducing interference and enhancing user transmission signals.

(2) A maximization EE algorithm is proposed. Based on the BCD algorithm, the EE problem is decomposed into three subproblems: optimizing the IRS phase shift matrix, power allocation, and UAV hovering position. Through iterative convergence improvement, the optimal EE target value is obtained. Simulation results show that the UAV-IRS integrated model significantly outperforms a single UAV model.

(3) An improved PSO algorithm is used to find the optimal hovering position of the UAV when approaching ground users, aiming to optimize UAV position to maximize EE and obtain an energy-saving UAV flight path.

The rest of this paper is organized as follows: Section 2 presents a system model for a UAV information acquisition system with IRS deployed on a stationary building, aiming to maximize energy efficiency. Section 3 formulates the problem of maximizing energy efficiency. In Section 4, the non-convex problem is transformed into a convex optimization problem, and the improved PSO algorithm and maximum energy efficiency algorithm are presented. Section 5 verifies the proposed algorithm through simulation. Section 6 summarizes and looks forward to the work of this paper.

2. Proposed model

2.1. System model

A communication scenario IRS-aided UAV information harvesting system is taken into consideration with uplink in Figure 1, where IRS is deployed in stationary building assisting in

transmitting information from multiple user equipments (UEs) to the single UAV. The cluster of UEs is denoted by $\mathcal{K} = \{1, \cdots, k, ..., K\}$. It is assumed that there exists an eavesdropper (Eve), and all K UEs, UAV, and Eve are equipped with a single antenna. In the three-dimensional (3D) cartesian coordinate system, the UE k is denoted by $w_k = [x_k, y_k, 0]$, where $k \in \mathcal{K}$. The coordinates of IRS and Eve are set as $w_r = [x_r, y_r, z_r]$ and $w_e = [x_e, y_e, 0]$, respectively. The flight period Γ of UAV is divided into N equally spaced time slots with step size $\triangle t$, i.e., $\Gamma = \triangle t N$. Denote $N = \{1, ..., n, ..., N\}$ as the set of all discrete time slots. The UAV flies at a fixed altitude H_{UAV} and $q[n] = [x_{UAV}[n], y_{UAV}[n], H_{UAV}]$ represents the coordinates of $i-$th stop point. The IRS is composed of a uniform planar array (UPA) with $C^{M \times M}$, where M expresses as the elements along the x-axis and z-axis. The diagonal phase-shift matrix of IRS is regarded as $\Phi \triangleq \left\{ \Phi[n] = diag(e^{j\theta_1[n]}, e^{j\theta_2[n]}, ..., e^{j\theta_m[n]}, ..., e^{j\theta_M[n]} \in C^{M \times M}, \forall n) \right\}$, where $\theta_i[n] \in [0, 2\pi), i \in \{1, ..., m, ..., M\}$ is the phase shift of the $i-$th reflecting element in time slot n.

Notations: In the work $(\cdot)^H$, $(\cdot)^T$ and $(\cdot)^{-1}$ stand for the Hermitian transpose, transpose, and inverse of matrix, respectively. Symbols $|\cdot|$ and $\|\cdot\|$ refer to the modulus and Euclidian norm of a complex number, and $\otimes$ is the Kronecker product.
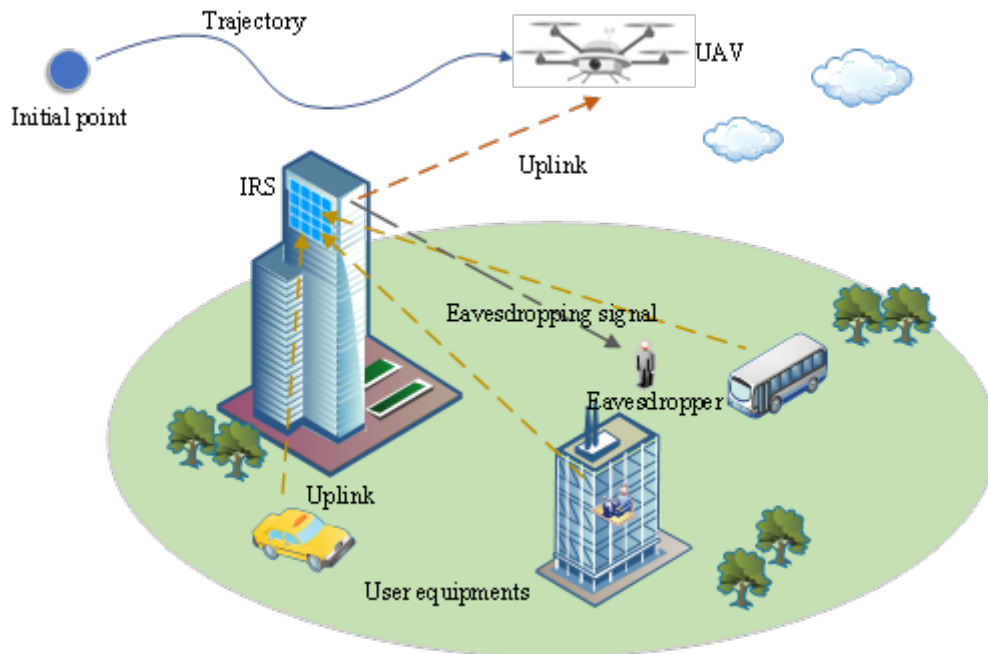

Figure 1. System model.

2.2. *Channel model*

It is assumed that there is non-LoS link between UAV and UEs [25]. The channel between UAV and UE k in time slot n can be modeled as

$$h_{uk}[n] = \sqrt{\frac{\rho_0}{d_{uk}^2[n]}} e^{-j\frac{2\pi}{\lambda}d_{uk}[n]}, \tag{2.1}$$

where $d_{uk}[n] = \left\| q[n] - w_k \right\|$ is the distance between the UAV and UE k, ρ_0 represents the path loss at the reference distance $d_0 = 1$ m, and λ is the carrier wavelength. Similarly, the channel between UAV

and Eve is modeled as

$$h_{ue}[n] = \sqrt{\frac{\rho_0}{d_{ue}^2[n]}} e^{-j\frac{2\pi}{\lambda}d_{ue}[n]}, \tag{2.2}$$

where $d_{ue}[n] = \left\| q[n] - w_e \right\|$ is the distance between the UAV and Eve.

Assume an LoS channel exists between the UAV and IRS, which can be modeled as

$$g_{ur}[n] = \sqrt{\frac{\rho_0}{d_{ur}^2[n]}}[1, e^{-j\frac{2\pi}{\lambda}d\varphi_{ur}[n]}, ..., e^{-j\frac{2\pi}{\lambda}d(M-1)\varphi_{ur}[n]}]^T, \tag{2.3}$$

where $d_{ur}[n] = \left\| q[n] - w_r \right\|$ is the distance between the IRS and UAV, d is the antenna spacing between adjacent reflection units, and $\varphi_{ur}[n] = \frac{x_{UAV}[n] - x_r}{d_{ur}[n]}$ represents the cosine of the angle of arrival (AoA) of signal from UAV to IRS.

The channel between IRS and UE k can be modeled as

$$g_{rk} = \sqrt{\frac{\rho_0}{d_{rk}^2}}[1, e^{-j\frac{2\pi}{\lambda}d\varphi_{rk}}, ..., e^{-j\frac{2\pi}{\lambda}d(M-1)\varphi_{rk}}]^T, \tag{2.4}$$

where $d_{rk} = \|w_r - w_k\|$ is the distance between the IRS and UE k, and $\varphi_{rk} = \frac{x_r - x_k}{d_{rk}}$ represents the cosine of the AoA of signal from UE k to IRS.

Similarly, the channel between IRS and Eve is modeled as

$$g_{re} = \sqrt{\frac{\rho_0}{d_{re}^2}}[1, e^{-j\frac{2\pi}{\lambda}d\varphi_{re}}, ..., e^{-j\frac{2\pi}{\lambda}d(M-1)\varphi_{re}}]^T, \tag{2.5}$$

where $d_{re} = \|w_r - w_e\|$ is the distance between the IRS and Eve, and $\varphi_{re} = \frac{x_r - x_e}{d_{re}}$ represents the cosine of the AoA of signal from Eve to IRS.

2.3. Signal model

The received signal in time slot n before power splitting can be given by

$$y_k[n] = \sqrt{p_k[n]}\left(g_{rk}^H[n]\Phi[n]g_{ur}[n]\right) + \sqrt{p_e[n]}\left(g_{re}^H[n]\Phi[n]g_{ur}[n]\right) + n_k, \tag{2.6}$$

where n_k denotes the additive white Gaussian noise (AWGN), p_e denotes the transmit power of Eve, and p_k denotes the transmit power of UE k. Let p_{max} and $\overline{p}$ represent the maximum transmit power and average transmit power of the UEs. The power constraints are

$$p_k[n] \le p_{max}, \forall k, n, \tag{2.7a}$$

$$\frac{1}{N}\sum_{n=1}^{N} a_k[n] \le \overline{p}, \forall k, n. \tag{2.7b}$$

Let $a_k[n]$ denote the association of UE k in time slot n, where $a_k[n] = 1$ expresses the UE k associated with UAV. The constraints are as follows:

$$\sum_{k=1}^{K} a_k[n] \le 1, \forall k, n, \tag{2.8a}$$

$$a_k[n] \in \{0, 1\}, \forall k, n. \tag{2.8b}$$

Then, the received signal-to-interference-plus-noise-ratio (SINR) at the UE k can be calculated as

$$\gamma_k = \frac{p_k[n]\left|g_{rk}^H[n]\Phi[n]g_{ur}[n]\right|^2}{p_e[n]\left|g_{re}^H[n]\Phi[n]g_{ur}[n]\right|^2 + \sigma^2}, \tag{2.9}$$

where σ^2 denotes the power of AWGN. Therefore, the achievable sum-rate from UE k to UAV via IRS in time slot n can be calculated as

$$R_k[n] = B\log_2(1 + \frac{p_k[n]\left|g_{rk}^H[n]\Phi[n]g_{ur}[n]\right|^2}{p_e[n]\left|g_{re}^H[n]\Phi[n]g_{ur}[n]\right|^2 + \sigma^2}), \tag{2.10}$$

where B denotes the system bandwidth. In the whole harvesting information process with UAV, the sum-rate of all UEs can be given by

$$R_{tot} = \sum_{k=1}^{K} \sum_{n=1}^{N} R_k[n]. \tag{2.11}$$

The energy consumption in process of information harvesting is taken into account, which include data reception consumption, IRS reflecting consumption, and UAV's flying and hovering consumption. In this process, it is assumed that the UAV information receiving time is $\alpha\Gamma$. First of all, the IRS reflection loss E_{IRS} depends on the properties and resolution of the reflective elements that provide effective phase shift to the incident signal, and can be expressed as:

$$E_{IRS} = M^2 P_m \Gamma, \tag{2.12}$$

where P_m represents the reflection consumption of IRS components that control the phase of the reflected signal when activated.

Furthermore, the propulsion energy consumption supporting the flight and hovering of UAV is expressed as E_{UAV},

$$E_{UAV} = \sum_{n=1}^{N} \left(c_1 \|v(n)\|^3 + \frac{c_2}{\|v(n)\|} \right), \tag{2.13}$$

where c_1 and c_2 are two parameters related to the weight of the UAV, wing area, air density, etc. $v(n)$ is the fixed flight speed of the UAV, defined as

$$v(n) = \frac{\|q[n+1] - q[n]\|}{\Delta t}. \tag{2.14}$$

Therefore, based on Eqs (2.12) and (2.13), the EE of the UAV information collection system can be modeled as:

$$EE = \frac{R_{tot}}{E_{IRS} + E_{UAV}}. \tag{2.15}$$

3. Problem formulation

In this section, an optimization problem that maximizes EE of the UAV is proposed via jointly design of the transmit power of UEs, the trajectory of UAV, and the phase shift matrix of IRS in the process of information harvesting. The problem is formulated as

$$
\begin{aligned}
&P1 : \max_{\mathbf{p},\mathbf{q},\Phi} EE, \\
&\text{s.t.} \ C1 : p_k[n] \leq p_{\max}, \forall k,n, \\
&\quad\ C2 : \frac{1}{N}\sum_{n=1}^{N} a_k[n] \leq \overline{p}, \forall k,n, \\
&\quad\ C3 : \sum_{k=1}^{K} a_k[n] \leq 1, \forall k,n, \\
&\quad\ C4 : a_k[n] \in \{0,1\}, \forall k,n, \\
&\quad\ C5 : R_k[n] \geq R_k^{\min}, \forall k,n, \\
&\quad\ C6 : \Phi = diag(e^{j\theta_1}, e^{j\theta_2}, ..., e^{j\theta_m}, ..., e^{j\theta_M}), 0 \leq \theta_m \leq 2\pi,
\end{aligned}
\tag{3.1}
$$

where $\mathbf{p} = \{p_1, \ldots p_k, \ldots p_K, p_e\}$ and $\mathbf{q} = \{q[n], \forall n\}$, C1 ensures the transmit power of UE k controlled on the maximum transmit power $p_{\max}$; C2 reflects the constraint on average transmit power $\overline{p}$ with UEs; C3 denotes the UAV's only link to a UE in time slot n; C4 represents whether the UAV is associated with UE k; C5 guarantees the sum rate situated above the minimum limit; and C6 ensures the unit modulus constraint for the passive beamforming with IRS.

4. Proposed algorithm

4.1. IRS phase shits optimization

To maximize the received signal energy, the phases beamforming matrix Φ is designed. The optimization problem can be rewritten as

$$
g_{rk}^{H}[n]\Phi[n]g_{ur}[n] = \frac{\rho_0 \sum\limits_{m=1}^{M} e^{j(\theta_m[n] + \frac{2(m-1)\pi d}{\lambda}(\varphi_{ur}[n] - \varphi_{rk}))}}{\sqrt{d_{rk}^2 d_{ur}^2[n]}}.
\tag{4.1}
$$

Combine signals from different paths at the UAV, and the phase of M elements with IRS is equivalent in time slot n. The formula result can be obtained:

$$
\begin{aligned}
\iota &= \theta_1[n] \\
&= \theta_2[n] + \frac{2\pi d}{\lambda}(\varphi_{ur}[n] - \varphi_{rk}) = ... \\
&= \theta_m[n] + \frac{2(m-1)\pi d}{\lambda}(\varphi_{ur}[n] - \varphi_{rk}) = ... \\
&= \theta_M[n] + \frac{2(M-1)\pi d}{\lambda}(\varphi_{ur}[n] - \varphi_{rk}).
\end{aligned}
\tag{4.2}
$$

The above equation obtains the optimized IRS phase shift matrix Φ^{opt}. The phase alignment of the received signal is realized and the received signal energy is further enhanced. Therefore, the phase shift of the $m-$th element in the IRS is represented as:

$$\theta_m[n] = \frac{2(m-1)\pi d}{\lambda}(\varphi_{rk} - \varphi_{ur}[n]) + \iota, \forall m, n, k. \tag{4.3}$$

Thus, $g_{rk}^H[n]\Phi[n]g_{ur}[n]$ can be rewritten as

$$g_{rk}^H[n]\Phi[n]g_{ur}[n] = \frac{\rho_0 M e^{j\iota}}{\sqrt{d_{rk}^2 d_{ur}^2[n]}}. \tag{4.4}$$

and $\left|g_{re}^H[n]\Phi[n]g_{ur}[n]\right|^2$ can be rewritten as

$$\left|g_{re}^H[n]\Phi[n]g_{ur}[n]\right|^2 = \frac{|\rho_0|^2 C^2}{d_{re}^2 d_{ur}^2[n]}, \tag{4.5}$$

where $C = \left|\sum_{m=1}^{M} e^{j(\theta_m[n] + \frac{2(m-1)\pi d}{\lambda}(\varphi_{re}[n] - \varphi_{ur}[n]))}\right|$.

In addition, the eavesdropper's channel gain is a complex function related to the trajectory of the UAV. For ease of calculation, its upper bound is set to:

$$\left|g_{re}^H[n]\Phi[n]g_{ur}[n]\right|^2 \leq \frac{|\rho_0|^2 M^2}{d_{re}^2 d_{ur}^2[n]}. \tag{4.6}$$

4.2. Power optimization

To solve optimization problem (P1), based on the calculated IRS phase shift matrix Φ^{opt} from the previous section and with the UAV trajectory q fixed, the power optimization problem can be simplified to:

$$P2 : \max_{\mathbf{p}} EE, \\ s.t.C1 - C6. \tag{4.7}$$

The problem ($P2$) is solved using the Dinkelbach algorithm as follows:

$$\mu^* = \max_{\mathbf{p}} \frac{R_{tot}}{E_{UAV}}, \tag{4.8}$$

where μ^* is a nonnegative parameter. Our objective is to update η at each iteration until it converges to η^* or reaches the maximum iteration value $J_{\max}$. Assuming the iteration index is J, the optimization problem of given parameters in each iteration is η^J. $P2$ can be expressed as:

$$\max_{\mathbf{p}}\{S(\mathbf{p}, \eta^J) = R_{tot}(\mathbf{p}) - \eta^J E_{UAV}(\mathbf{p})\}, \\ s.t.C1 - C6. \tag{4.9}$$

Formula (4.9) can be obtained through simple mathematical processing, which leads to the following equation:

$$f_1(\mathbf{p}) = B \sum_{k=1}^{K} \sum_{n=1}^{N} \log_2(p_k[n]\left|g_{rk}^H[n]\Phi[n]g_{ur}[n]\right|^2 + p_e[n]\left|g_{re}^H[n]\Phi[n]g_{ur}[n]\right|^2 + \sigma^2), \tag{4.10}$$

$$f_2(\mathbf{p}) = B \sum_{n=1}^{N} \log_2(p_e[n]\left|g_{re}^H[n]\Phi[n]g_{ur}[n]\right|^2 + \sigma^2) + \eta^J(E_{IRS} + E_{UAV}), \tag{4.11}$$

where both $f_1(\mathbf{p})$ and $f_2(\mathbf{p})$ are convex functions. Function $f_2(\mathbf{p})$ can be approximated as $f_2(\mathbf{p}^J) + \nabla f_2(\mathbf{p}^J)(\mathbf{p} - \mathbf{p}^J)$ through the first-order Taylor expansion [26]. $\nabla f_2(\mathbf{p}^J)$ represents the gradient of $f_2(\mathbf{p})$ at point $\mathbf{p}^J$, and its calculation formula is

$$\nabla f_2(\mathbf{p}^J) = B \sum_{n=1}^{N} \frac{1}{\left(\left|g_{re}^H[n]\Phi[n]g_{ur}[n]\right|^2 + \sigma^2\right)\ln 2}. \tag{4.12}$$

Therefore, the objective function can be further transformed into

$$\max_{\mathbf{p}}\{S(\mathbf{p}^J) = f_1(\mathbf{p}) - f_2(\mathbf{p}) - \nabla f_2(\mathbf{p}^J)(\mathbf{p} - \mathbf{p}^J)\},$$
$$\text{s.t.C1} - \text{C6}. \tag{4.13}$$

According to the above steps, the power allocation process is transformed into Algorithm 4.1 as follows:

Algorithm 4.1 Power Allocation Algorithm

Initialization: Set iteration index $J = 0$, maximum number of iterations $J_{\max}$, and tolerance value $\varepsilon \ll 1$.

repeat

    For a given η^0 and $\mathbf{p}^J$, compute equivalent problem(4.9) to obtain the optimal solution $\mathbf{p}^{opt}$.

    Make $\mathbf{p}^J = \mathbf{p}^{opt}$ and calculate $S(\mathbf{p})$.

    $J = J + 1$

until the iteration index $J > J_{\max}$ or $|S(\mathbf{p})| \leq \varepsilon$.

make $\mathbf{p}^0 = \mathbf{p}^J, \eta^0 = \eta^J$.

4.3. Trajectory optimization

In this section, aiming at maximizing EE, the improved PSO algorithm is used to find the optimal hover point based on the power $\mathbf{p}^{opt}$ and IRS phase shift matrix Φ^{opt} obtained in the previous two sections, so as to optimize the position of the UAV and find the shortest path in the flight process of the UAV.

The inertia factor in PSO has an important impact on the performance and search ability of the entire algorithm. A larger inertia factor can increase the velocity change of particles, enabling them to jump out of local optimal solutions and obtain better global search ability. A smaller inertia factor can reduce the velocity change of particles, making them more inclined toward local search. Therefore, in the early stage of the algorithm search process, we first perform wide-range search, then quickly determine the range where the global optimum is located, and finally use local search to determine a

highly accurate solution. During the process of solving optimization problems, it should be ensured that the inertia weight decreases continuously with the increase of iterations [27]. Therefore, in this work, the inertia factor ω is introduced to achieve a balance between convergence speed and local search ability, which is expressed as:

$$\omega = \omega_{\max} - (\omega_{\max} - \omega_{\min})\frac{r}{r_{\max}}. \tag{4.14}$$

in which $\omega_{\max}$ and $\omega_{\min}$ are the maximum and minimum values of the inertia weight coefficient, typically set as $\omega_{\max} = 0.9$, $\omega_{\min} = 0.4$. The r represents the current iteration number, and $r_{\max}$ represents the maximum iteration number value. The particle exhibits strong nonlinearity in the search process. The inertia weight must be set according to the distance of the global optimal position and the number of iterations to balance the relationship between search speed and search accuracy. As a result, the inertia weight can fully adapt to changes in the number of search iterations, improving the overall search capability [28]. Therefore, this section proposes an improved nonlinear inertia weight, dynamically adjusting the inertia factor in the algorithm search process, denoted as:

$$\omega = \omega_{\max} - (\omega_{\max} - \omega_{\min}) \times [\frac{2r}{r_{\max}} - (\frac{r}{r_{\max}})^2]. \tag{4.15}$$

In addition, the learning factor is one of the important parameters that control the adaptive search behavior of particles. In traditional PSO algorithms, a fixed learning factor is used, which is usually a constant set through experience. Due to the randomness of the search process, it becomes very difficult to accurately quantify the relationship between the coefficient value and the number of iterations. In order to ensure that the path planning search of particles obtains enough path nodes and the population converges continuously to obtain the global optimal solution, the first half of the search process is considered dominant in the calculation process, while the second half is dominated by convergence [29]. Therefore, the adaptive parameters c_1' and c_2' are improved as:

$$c_1' = c_{\max} - \frac{(c_{\max} - c_{\min})r}{r_{\max}}, \tag{4.16}$$

$$c_2' = c_{\min} + \frac{(c_{\max} - c_{\min})r}{r_{\max}}. \tag{4.17}$$

It is clear that c_1' presents a linear decrease and c_2' presents a linear increase, with the sum of $(c_1' + c_2')$ being constant, indicating that the search and convergence ability of particles is constant. $c_{\max}$, $c_{\min}$ are constant values and $c_{\max} > c_{\min} > 0$. In the search phase of PSO, $c_1' > c_2'$ is satisfied, which enhances the ability of particles to search for path nodes and avoids falling into local minima. In the convergence phase of PSO, $c_1' < c_2'$ is satisfied, enabling particles to quickly converge to the global optimal solution. Therefore, the velocity update and position update formulas for particle swarm are as follows:

$$v_k[r + 1] = \varpi v_k[r] + c_1' s_1(p_{bk}[r] - x_k[r]) + c_2' s_2(g_b[r] - x_k[r]) \tag{4.18}$$

$$x_k[r + 1] = x_k[r] + v_k[r + 1]. \tag{4.19}$$

in which $v_k[r + 1]$ represents the velocity of particle k at the $[r + 1]-$th iteration, $v_k[r]$ represents the velocity of particle k at the $r-$th iteration, $x_k[r]$ represents the position of particle k at the $r-$th iteration,

and s_1 and s_2 represent weights between 0 and 1. $p_{bk}[r]$ and $g_b[r]$ are the historical extreme value of individual k and population at the $r-$th iteration, respectively.

When PSO is used to solve the UAV's track planning problem, the best location of the track space is planned. The essence of track coding is to establish a one-to-one mapping relationship between each particle in the population and each iteration candidate track in the search space [30].

Algorithm 4.2 Improved PSO Algorithm Based on UAV EE Maximization

---

Input: The coordinates of the UE in the given area are $w_k = [x_k, y_k, 0]$, where $k \in \mathcal{K}$; the positions of the IRS and eavesdropper are $w_r = [x_r, y_r, z_r]$ and $w_e = [x_e, y_e, 0]$, respectively; the phase shift matrix of the IRS is Φ^{opt}; the flight power of the UAV is p^{opt}. Set the iteration index to $r = 0$ and the maximum number of iterations to $r_{\max}$.

Output: UAV Hovering Point $q^{opt} = [x_{UAV}, y_{UAV}, H_{UAV}]$

1: Calculation of UAV hover coordinate $q^* = [x^*, y^*, H]$ under problem (4.13) based on IRS technique.
2: Initialization: Set the number of particles in the solution space to k, inertia weight to ω, learning factors to c'_1 and c'_2; set particle positions and impose spatial constraints.
3: Calculate the objective function value corresponding to the particle based on Eq (4.13), and calculate the optimal individual extreme value of the particle based on Eq (4.19).
4: **Loop repetition**
5: Update the velocity information of the particles based on Eq (4.18); Update the position information of the particles based on Eq (4.19).
6: Update the fitness function value based on Eq (4.20).
7: Compare the fitness value obtained in step (6) with the fitness value corresponding to the best individual's extremum, and update the particle's best position information based on Eq (4.23).
8: Compare the fitness value of the best individual's extremum obtained in Step (7) with the fitness value of the global extremum, and update the global best position information based on Eq (4.24).
9: $r = r + 1$
10: Until iteration index $r > r_{\max}$ or $|S(\mathbf{p}^r) - S(\mathbf{p}^{r-1})| \leq \varepsilon$.
11: make $q^* = q^{opt}$, $EE^* = EE^{opt}$.

In addition, in the PSO algorithm, fitness is used to evaluate the quality of each particle's position in the search space, measuring the particle's ability or performance in problem-solving. Considering the distance between UAV and users in this research problem, the fitness function expression is set as:

$$f_v[r] = \sum_{n=1}^{N} \sum_{k=1}^{K} \sqrt{(x_{UAV}[r] - x_k)^2 + (y_{UAV}[r] - y_k)^2 + (H_{UAV}[r] - 0)^2}. \tag{4.20}$$

In the process of iterative search, PSO tracks and studies two extreme values, namely, the optimal solution obtained by the particle itself and the optimal solution obtained by the particle swarm, which is mainly used to complete the optimization analysis of the problem [27].

Assume the individual extreme value searched by the $k-$th particle is

$$p_{best} = (p_{b1}, p_{b2}, ..., p_{bK}). \tag{4.21}$$

The global extreme value found by the entire particle swarm is

$$g_{best} = (p_{g1}, p_{g2}, ..., p_{gK}). \tag{4.22}$$

After r−th iterations, following Eqs (4.19) and (4.20),

$$p_{best}(r + 1) = \begin{cases} p_{best}(r + 1), & f[p_{best}(r + 1)] \geq f[p_{best}(r)] \\ p_{best}(r), & f[p_{best}(r + 1)] < f[p_{best}(r)] \end{cases} \tag{4.23}$$

$$g_{best}(r + 1) = \begin{cases} g_{best}(r + 1), & f[g_{best}(r + 1)] \geq f[g_{best}(r)] \\ g_{best}(r), & f[g_{best}(r + 1)] < f[g_{best}(r)] \end{cases} \tag{4.24}$$

In the above equation, the particle continuously updates individual best and global best values during the iteration process. If $f[p_{best}(r + 1)] \geq f[p_{best}(r)]$, it means that it has found a position with better fitness than before; if $f[p_{best}(r + 1)] < f[p_{best}(r)]$, it means that the current individual's best position is not as good as the previous one.

According to the above formula, based on the maximization EE problem described in Eq (4.13), the improved PSO algorithm is used to solve for the coordinates of the optimal hovering point for the UAV, and the process of obtaining the UAV's flight trajectory is shown in Algorithm 4.2.

According to Algorithm 4.2, the coordinates of the best hover point for the UAV in the flight area and the corresponding optimal EE are calculated. These coordinate points serve as the access points for the UAV, connecting with each other based on maximizing EE, forming the order of the UAV's access communication devices and thus shaping the UAV's flight trajectory.

Algorithm 4.3 Maximize EE Algorithm

1: Initialization: Set the EE optimization value η^0, the iteration index $a = 0$, the maximum number of iterations $a_{\max}$, and the tolerance value $\varepsilon \ll 1$.
2: **Loop repetition**
3: Obtain the IRS phase shift matrix Φ^{opt} through phase shift optimization based on the given power $\mathbf{p}$ and UAV trajectory q.
4: Obtain the power $\mathbf{p}^{opt}$ through Algorithm 4.1 based on the IRS phase shift matrix Φ^{opt} obtained by the given UAV trajectory q and Step (3).
5: Obtain the UAV trajectory q^{opt} through Algorithm 4.2 based on the IRS phase shift matrix Φ^{opt} obtained in Step (3) and the power $\mathbf{p}^{opt}$ obtained in Step (4).
6: update $\eta^{opt} = \eta^a$.
7: $a = a + 1$
8: Until the iterative index $a > a_{\max}$ or $\left| S(\mathbf{p}^J) - S(\mathbf{p}^{J-1}) \right| \leq \varepsilon$.
9: output $\eta^* = \eta^{opt}$

4.4. Transformation of the problem

Based on the BCD algorithm, this research decomposes the problem of maximizing EE into three subproblems: IRS phase shift optimization, power optimization, and UAV trajectory optimization. By dividing the subproblems step by step using the basic algorithm principles and setting iterative

indicators and upper bounds, the convergence of the overall algorithm is ensured. Based on the three subproblems in the above chapters, this section designs the overall problem as a maximization algorithm for EE. The specific implementation process is shown in Algorithm 4.3, where the algorithm complexity of Step (4) is denoted as $O(NJ)$, and the algorithm complexity of Step (5) is denoted as $O(NJ + Kr)$. The algorithm flow of overall is shown in Figure 2 below.
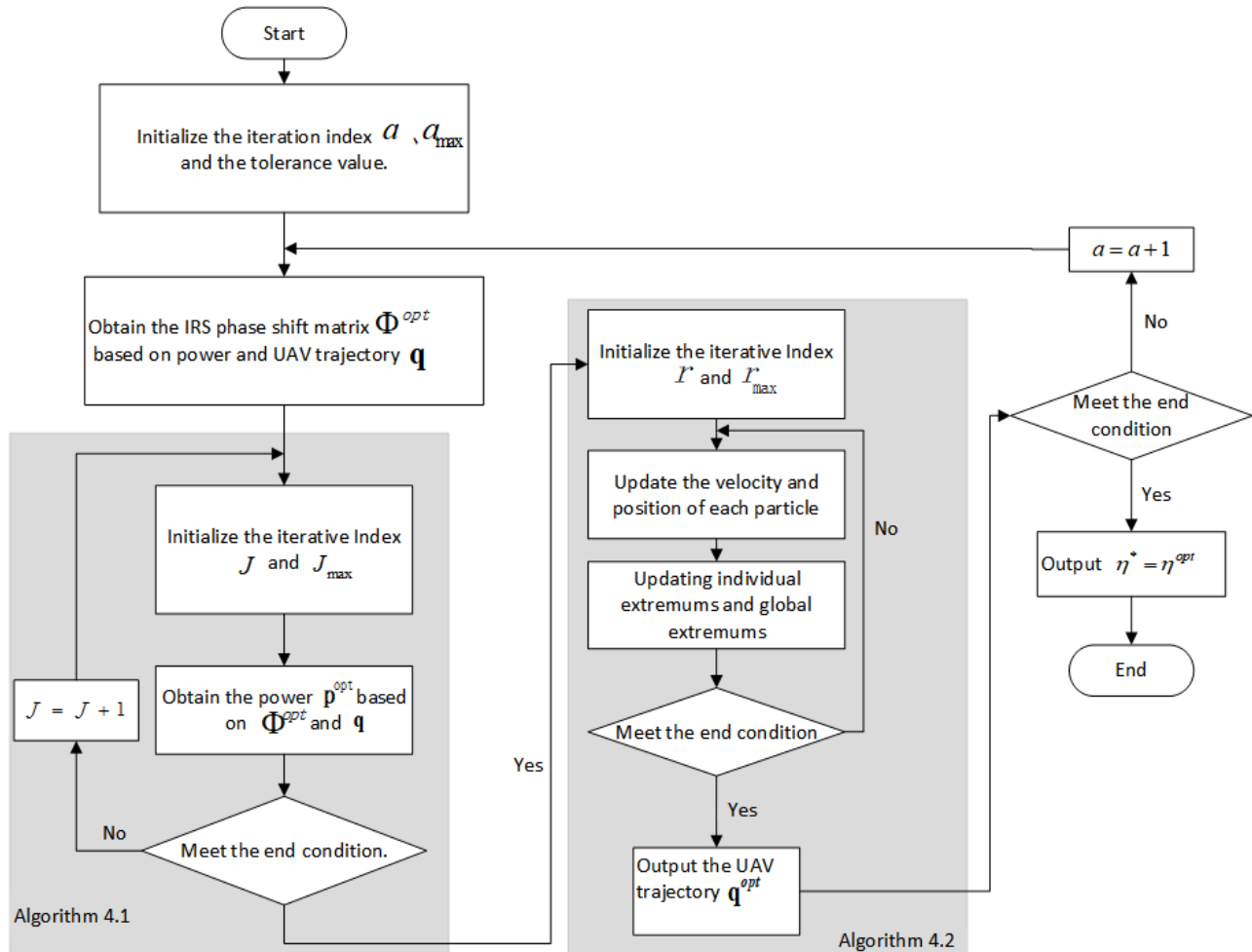

Figure 2. Algorithm flow of overall.

5. Simulation results and analysis

In this section, the effectiveness of the proposed algorithm is evaluated through simulation experiment results. It is assumed that all UEs are randomly distributed in suburban environments, with actual noise variance as $\sigma^2 = -110$ dBm, fault tolerance value as $\delta = 1 \times 10^{-4}$, channel gain at interference distance $d_0 = 1$m as $\beta_0 = -50$ dB, maximum value of inertia weight coefficient as $\omega_{max} = 0.9$, and minimum value of inertia weight coefficient as $\omega_{min} = 0.4$. This study considers the scenario where a single UAV collaborates with IRS to establish the channel and collect information from ground users. To begin, by changing the numerical values of the UAV's flight altitude and P_{max},

the changes in UAV efficiency under four different scenarios of UAV only, UAV-IRS integration, GA improved based on UAV-IRS integration, and PSO algorithm improved based on UAV-IRS integration are studied through multiple alternating iterations, validating the superior performance of the UAV-IRS integrated improved PSO algorithm over the other scenarios. Additionally, the changes in UAV efficiency with a fixed altitude and P_{max} and varying the number of IRS reflecting units are studied. Then, based on the improved PSO algorithm, the optimal hovering position for UAV is calculated, and an efficient and energy-saving flight trajectory for the UAV is designed. Finally, changes in fitness during the process of solving the optimal hovering position using the improved PSO algorithm are explored by varying the number of alternating iterations.
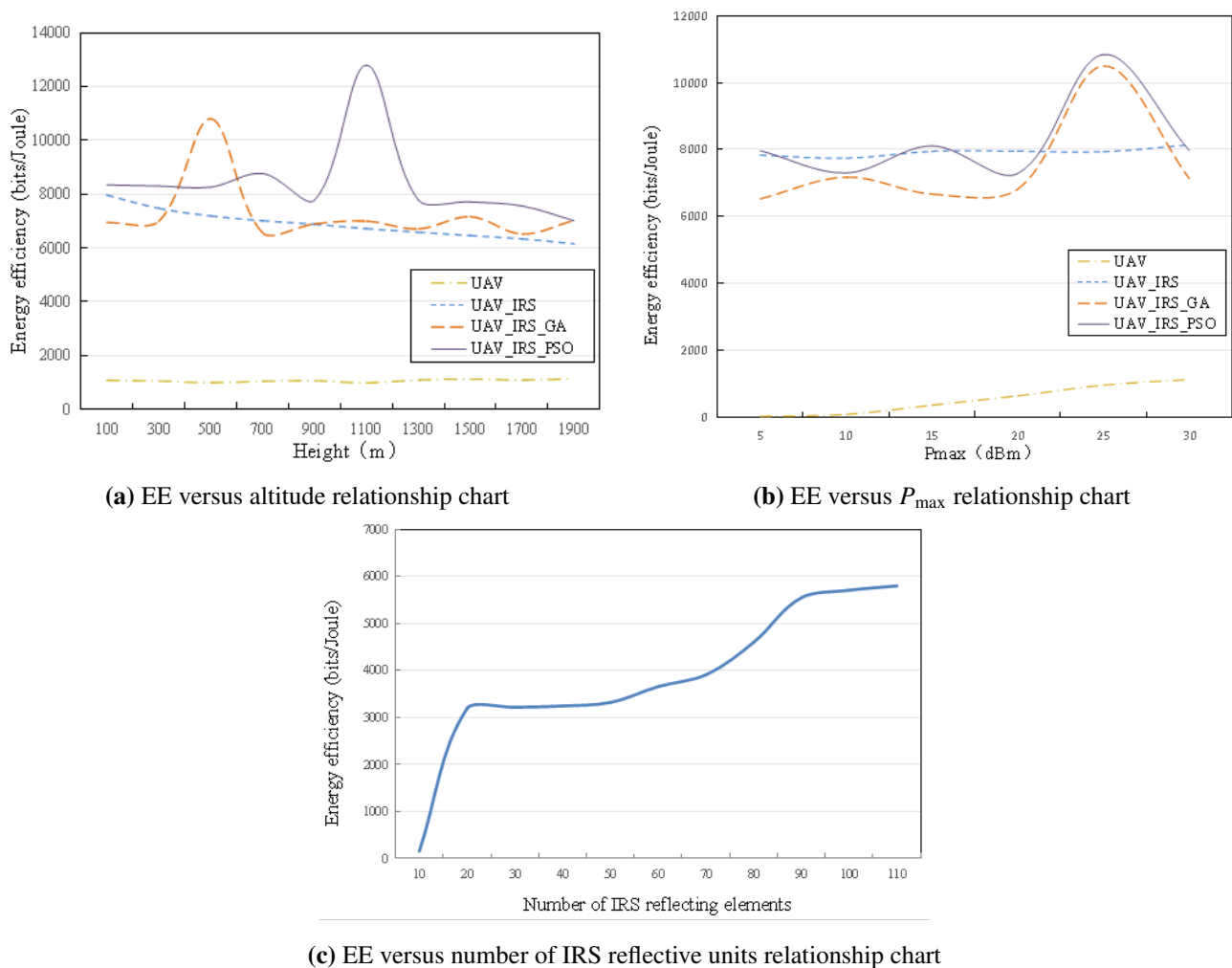

(a) EE versus altitude relationship chart

(b) EE versus P_{max} relationship chart

(c) EE versus number of IRS reflective units relationship chart

Figure 3. EE change chart.

This section simulates the communication service scenario where UAVs fly in the user-demand area to collect ground UE information, and the comparison of the proposed algorithm under different parameters is shown in Figure 3. Figure 3(a) illustrates the superiority of the collaborative scheme combining IRS phase optimization, power optimization, and UAV trajectory optimization as in Algorithm 4.3. To start, the maximum power of the UAV is fixed at $P_{max} = 25$ dBm. On the one hand,

under the same UAV-IRS integrated improved PSO algorithm, the system efficiency increases with the increase of UAV flight altitude and reaches the EE maximization of uav at altitude $H = 1150m$. Subsequently, as the distance between the UAV and ground users becomes too high, leading to a weakening of the communication channel performance, the efficiency value decreases and gradually converges. On the other hand, the EE performance of the UAV-IRS integrated improved PSO algorithm is better than the other three cases in the figure, demonstrating the superiority of the algorithm proposed in this chapter: UAV-IRS integrated improved PSO algorithm > UAV-IRS integrated improved GA algorithm > UAV-IRS integrated > UAV only. Additionally, the EE performance of the PSO algorithm based on IRS improvement is more than 22% higher than that of the GA algorithm based on IRS improvement. Figure 3(b) shows the variation of UAV EE with parameter $P_{\max}$ as the UAV flight altitude is $H = 100m$. Figure 3(c) illustrates the variation of UAV system EE with changes in the number of IRS reflecting units. According to the simulation experiment results, the EE continuously increases with the increase of the number of IRS reflecting units M gradually after $M = 86$, and eventually reaches equilibrium.
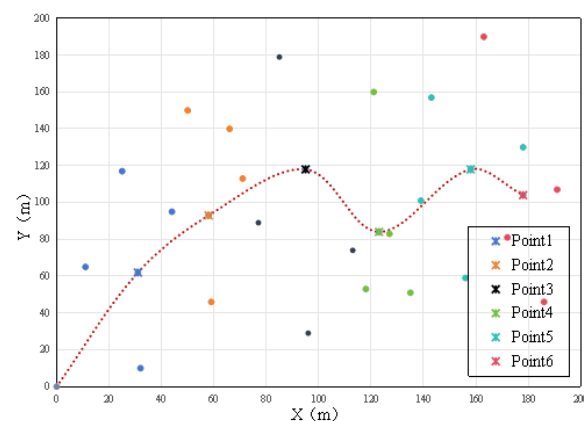
(a) The horizontal flight trajectory map of the UAV
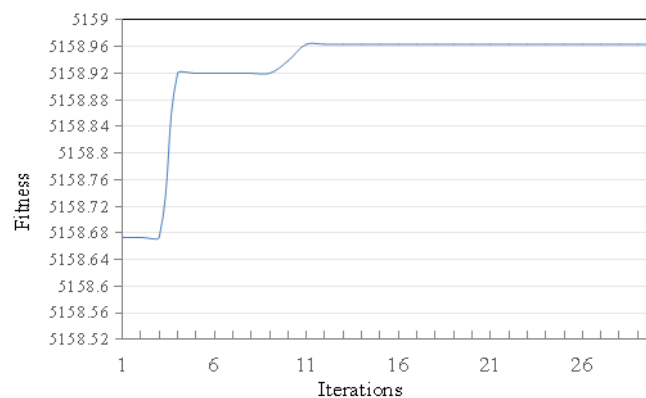
(b) The fitness vs. iteration number

Figure 4. UAV flight trajectory and its fitness variation graph.

According to Algorithm 4.2, the improved PSO algorithm for UAV-IRS integration was studied based on fixed UAV flight altitude and transmission power. As shown in Figure 4(a), the randomly

scattered colored dots represent the distribution of UEs in area $200\ m \times 200\ m$. The UAV flies from the initial point $(0\ m, 0\ m)$ at the initial velocity $30\ m/s$, while UEs move at speed $10\ m/s$. According to the goal of maximizing the EE of the UAV, the UAV sequentially hovers at the calculated optimal hover point positions to collect the transmission information required by UEs in this area, forming a high-efficiency flight trajectory in a simulated scenario. The number of UEs is set as $K = 24$. In addition, during the UAV flight process, Figure 4(b) studies the fitness changes of Algorithm 4.2. With the increase of the number of alternating iterations, the fitness value of the UAV communication task increases rapidly and converges quickly around 11 times, reaching the threshold value of the cluster fitness value, which shows that the global convergence of the algorithm proposed in this section is better, it can effectively avoid the PSO algorithm searching to fall into the local stagnation dilemma, and it can improve the quality of the UAV flight trajectory effectively, with shorter time-consumption and better stability.

6. Conclusions

In this paper, we studied a UAV information collection system based on IRS. Considering the mobility of ground users and the interference signals from eavesdroppers, we incorporated the technical advantages of IRS to construct a new UAV wireless communication channel and established a UAV channel model based on IRS to mitigate interference and enhance the transmission signal of users themselves. Then, according to the BCD algorithm, the EE problem was decomposed into three subproblems, optimizing the IRS phase shift matrix, power allocation, and UAV hovering position. Through PSO improved algorithms, the optimal EE objective value was obtained. Simulation results show that the UAV-IRS integrated model in this study outperforms the UAV model alone significantly, which helps improve issues such as wireless channel fading in UAV-assisted wireless communication and enhances the transmission quality of communication tasks.

Use of AI tools declaration

The authors declare they have not used Artificial Intelligence (AI) tools in the creation of this article.

Conflict of interest

The authors declare there is no conflicts of interest.

References

1. A. Sonny, S. R. Yeduri, L. R. Cenkeramaddi, Autonomous UAV path planning using modified PSO for UAV-assisted wireless networks, *IEEE Access*, **2023** (2023). https://doi.org/10.1109/ACCESS.2023.3293203

2. C. Pan, G. Zhou, K. Zhi, S. Hong, T. Wu, Y. Pan, et al., An overview of signal processing techniques for RIS/IRS-aided wireless systems, *IEEE J. Sel. Top. Signal Process.*, **16** (2022), 883–917. https://doi.org/10.1109/JSTSP.2022.3195671

3. C. You, Z. Kang, Y. Zeng, R. Zhang, Enabling smart reflection in integrated air-ground wireless network: IRS meets UAV, *IEEE Wireless Commun.*, **28** (2021), 138–144. https://doi.org/10.1109/MWC.001.2100148

4. A. Mahmoud, S. Muhaidat, P. C. Sofotasios, I. Abualhaol, O. A. Dobre, H. Yanikomeroglu, et al., Intelligent reflecting surfaces assisted UAV communications for IoT networks: Performance analysis, *IEEE Trans. Green Commun. Networking*, **5** (2022), 1029–1040. https://doi.org/10.1109/TGCN.2021.3068739

5. X. Liu, Y. Liu, Y. Chen, Machine learning empowered trajectory and passive beamforming design in UAV-RIS wireless networks, *IEEE J. Sel. Areas Commun.*, **39** (2021). https://doi.org/10.1109/JSAC.2020.3041401

6. W. Yu, J. Liu, J. Zhou, A novel sparrow particle swarm algorithm (SPSA) for unmanned aerial vehicle path planning, *Sci. Program.*, **2021** (2021), 1–15. https://doi.org/10.1155/2021/5158304

7. X. Zhou, F. Gao, X. Fang, Z. Lan, Improved bat algorithm for UAV path planning in three-dimensional space, *IEEE Access*, **9** (2021), 20100–20116. https://doi.org/10.1109/ACCESS.2021.3054179

8. Q. Deng, Integrated planning of UAV 3D trajectory based on ant colony algorithm, in *Journal of Physics: Conference Series*, **2330** (2022). https://doi.org/10.1088/1742-6596/2330/1/012009

9. Y. Su, X. Pang, S. Chen, X. Jiang, N. Zhao, F. R. Yu, Spectrum and energy efficiency optimization in IRS-assisted UAV networks, *IEEE Trans. Commun.*, **70** (2022), 6489–6502. https://doi.org/10.1109/TCOMM.2022.3201122

10. X. Song, Y. Zhao, Z. Wu, Z. Yang, J. Tang, Joint trajectory and communication design for irs-assisted uav networks, *IEEE Wireless Commun. Lett.*, **11** (2022), 1538–1542. https://doi.org/10.1109/LWC.2022.3179028

11. H. Long, M. Chen, Z. Yang, Z. Li, B. Wang, X.Yun, et al., Joint trajectory and passive beamforming design for secure UAV networks with RIS, in *2020 IEEE Globecom Workshops*, (2020), 1–6. https://doi.org/10.1109/GCWkshps50303.2020.9367542

12. Z. Ji, W. Yang, X. Guan, X. Zhao, G. Li, Q. Wu, Trajectory and transmit power optimization for IRS-assisted UAV communication under malicious jamming, *IEEE Trans. Veh. Technol.*, **71** (2022), 11262–11266. https://doi.org/10.1109/TVT.2022.3187092

13. X. Mu, Y. Liu, L. Guo, J. Lin, H. V. Poor, Intelligent reflecting surface enhanced multi-UAV NOMA networks, *IEEE J. Sel. Areas Commun.*, **39** (2021), 3051–3066. https://doi.org/10.1109/JSAC.2021.3088679

14. H. Shakhatreh, A. Sawalmeh, A. H. Alenezi, S. Abdel-Razeq, A. Al-Fuqaha, Mobile-IRS assisted next generation UAV communication networks, *Comput. Commun.*, **215** (2024), 51–61. https://doi.org/10.1016/j.comcom.2023.12.025

15. M. Diamanti, M. Tsampazi, E. E. Tsiropoulou, S. Papavassiliou, Energy efficient multi-user communications aided by reconfigurable intelligent surfaces and UAVs, *IEEE International Conference on Smart Computing (SMARTCOMP)*, (2021), 371–376. https://doi.org/10.1109/SMARTCOMP52413.2021.00075

16. X. Zhang, H. Zhang, W. Du, K. Long, A. Nallanathan, IRS empowered UAV wireless communication with resource allocation, reflecting design and trajectory optimization, *IEEE Trans. Wireless Commun.*, **21** (2022), 7867–7880. https://doi.org/10.1109/TWC.2022.3162704

17. N. Lin, H. Tang, L. Zhao, S. Wan, A. Hawbani, M. Guizani, A PDDQNLP algorithm for energy efficient computation offloading in UAV-assisted MEC, *IEEE Trans. Wireless Commun.*, **22** (2023), 8876–8890. https://doi.org/10.1109/TWC.2023.3266497

18. J. Yu, X. Liu, Y. Gao, C. Zhang, W. Zhang, Deep learning for channel tracking in IRS-assisted UAV communication systems, *IEEE Trans. Wireless Commun.*, **21** (2022), 7711–7722. https://doi.org/10.1109/TWC.2022.3160517

19. S. M. M. Abohashish, R. Y. Rizk, E. I. Elsedimy, Trajectory optimization for UAV-assisted relay over 5G networks based on reinforcement learning framework, *EURASIP J. Wireless Commun. Networking*, **2023** (2023), 55. https://doi.org/10.1186/s13638-023-02268-x

20. Y. Ullah, M. Roslee, S. M. Mitani, M. Sheraz, F. Ali, A. F. Osman, et al., Reinforcement learning-based unmanned aerial vehicle trajectory planning for ground users' mobility management in heterogeneous networks, *J. King Saud Univ. Comput. Inf. Sci.*, **36** (2024), 102052. https://doi.org/10.1016/j.jksuci.2024.102052

21. M. Ejaz, J. Gui, M. Asim, M. ElAffendi, C. Fung, A. A. Abd El-Latif, RL-Planner: Reinforcement learning-enabled efficient path planning in multi-UAV MEC systems, *IEEE Trans. Network Serv. Manage.*, **2024** (2024). https://doi.org/10.1109/TNSM.2024.3378677

22. L. Wang, K. Wang, C. Pan, N. Aslam, Joint trajectory and passive beamforming design for intelligent reflecting surface-aided UAV communications: A deep reinforcement learning approach, *IEEE Trans. Mobile Comput.*, **22** (2022), 6543–6553. https://doi.org/10.1109/TMC.2022.3200998

23. P. Huang, Y. Wang, K. Wang, Energy-efficient trajectory planning for a multi-UAV-assisted mobile edge computing system, *Front. Inf. Technol. Electron. Eng.*, **21** (2020), 1713–1725. https://doi.org/10.1631/FITEE.2000315

24. K. Zhi, C. Pan, H. Ren, K. K. Chai, M. Elkashlan, Active RIS versus passive RIS: Which is superior with the same power budget?, *IEEE Commun. Lett.*, **26** (2022), 1150–1154. https://doi.org/10.1109/LCOMM.2022.3159525

25. S. Li, B. Duo, X. Yuan, Y. C. Liang, M. Di Renzo, Reconfigurable intelligent surface assisted UAV communication: Joint trajectory design and passive beamforming, *IEEE Wireless Commun. Lett.*, **9** (2020), 716–720. https://doi.org/10.1109/LWC.2020.2966705

26. M. Alzenad, A. El-Keyi, H. Yanikomeroglu, 3-D placement of an unmanned aerial vehicle base station for maximum coverage of users with different QoS requirements, *IEEE Wireless Commun. Lett.*, **7** (2017), 38–41. https://doi.org/10.1109/LWC.2017.2752161

27. Y. An, Z. Zhang, W. Wu, Study on the UAV trajectory planning route based on the particle group optimization algorithm, in *2022 4th International Conference on Applied Machine Learning (ICAML)*, (2022), 184–187. https://doi.org/10.1109/ICAML57167.2022.00042

28. L. Li, X. Yang, Inspection path optimization of the agricultural unmanned aerial vehicle based on the improved PSO algorithm, *J. Eng. Sci. Technol. Rev.*, **16** (2023), 38–41. https://doi.org/10.25103/jestr.165.11

29. S. Shao, Y. Peng, C. He, Y. Du, Efficient path planning for UAV formation via comprehensively improved particle swarm optimization, *ISA Trans.*, **97** (2020), 415–430. https://doi.org/10.1016/j.isatra.2019.08.018

30. H. Cao, H. Zhang, Z. Liu, Y. Zhou, Y. Wang, UAV path planning based on improved particle swarm algorithm, in *2021 7th International Symposium on Mechatronics and Industrial Informatics (ISMII)*, IEEE, (2021), 284–287. https://doi.org/10.1109/ISMII52409.2021.00067

AIMS Press